Dual-plane ensemble correlation for pixelwise 2D-3C velocity field measurements using a single camera

D. Noto · Y. Tasaka

Abstract As an extension of single-pixel particle image velocimetry (SP-PIV), a novel method to determine both the out-of-plane and in-plane velocity fields with single-pixel resolution is presented. With this approach, called dual-plane SP-PIV, mean velocity vector fields with three components (3C) can be measured with single-pixel resolution using a single-color camera and two differently colored laser sheets. The method computes the ensemble correlation across two planes illuminated simultaneously by the two laser sheets. The method is demonstrated via an experiment in which a rotating flow is induced by an impeller. The method is validated by comparing its results with those of conventional PIV. The results show good accordance in terms of the magnitudes and spatial distributions of the out-of-plane velocities and provide a new approach to 3C velocity field measurements with high spatial resolution.

Keywords Single-pixel PIV · Dual-plane PIV · Rotating flow

1 Introduction

Single-pixel particle image velocimetry (SP-PIV) was first introduced by Westerweel et al. (2004) to measure mean velocity fields with single-pixel resolution, and it has since been extended to enable the measurement of unsteady and turbulent flows (Kähler et al. 2006; Scharnowski et al. 2012; Ozawa et al. 2020; Nonomura et al. 2020). SP-PIV is based on single-pixel ensemble correlation, which computes pixelwise cross-correlation

D. Noto · Y. Tasaka
Laboratory for Flow Control, Faculty of Engineering, Hokkaido University, Sapporo, Japan
E-mail: noto@ring-me.eng.hokudai.ac.jp

maps using temporal brightness signals extracted from sequential particle images, unlike the conventional PIV using image pairs. Thus, it can be further extended to measure the out-of-plane velocity component by adopting the idea of dual-plane PIV, which was earlier introduced by Cenedese and Paglialunga (1989) and Gharib et al. (1995). Dual-plane PIV determines the out-of-plane velocity component using only a single camera and multiple sheet illuminations at different depths. This method computes spatio-temporal correlations across multiple illuminated planes. We incorporated this idea into SP-PIV by implementing two parallel laser sheets with different colors to determine both the in-plane and out-of-plane velocity fields with single-pixel resolution. We moreover demonstrate its feasibility with a preliminary test experiment.

2 Principle

A conceptual image of the proposed method, called dual-plane ensemble correlation, is shown in Fig. 1. We consider a situation in which two adjoining planes with a depth offset Δz are illuminated by two light sheets with different colors, and the particle images in the two planes are correctly separated into foreside $\mathbf{I}_f$ and backside images $\mathbf{I}_b$ in advance. If these illuminated planes are sufficiently large, a particle with a considerable out-of-plane velocity appearing on one plane should also appear on the other plane. The idea of ensemble correlation in SP-PIV thus can be applied to the temporal brightness signals across the two planes. Consider a situation in which a particle passes a position $\mathbf{x}_0 = (x_0, y_0)$ in one plane at frame $t = t_0$. If the out-of-plane velocity at $\mathbf{x}_0$ is not negligible, this particle appears at $\mathbf{x}_\zeta$ in the other plane before or after $t = t_0$ at a different frame $t = t_\zeta =$
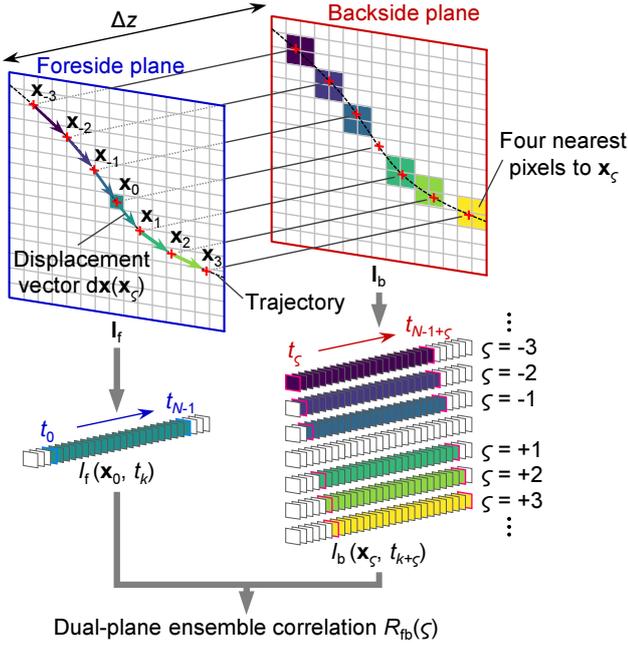
Fig. 1 Conceptual image of the dual-plane ensemble correlation.

$t_0 + \zeta \Delta t$ depending on the direction of the out-of-plane velocity. Here, ζ is an integer $\zeta = \pm 1, \pm 2 \ldots$ representing the frame offset and Δt is the time interval of the image acquisition. That is, we can prepare associated pairs of brightness signals extracted from sequential images in the two planes, i.e., $I_\mathrm{f}(\mathbf{x}_0, t)$ and $I_\mathrm{b}(\mathbf{x}_\zeta, t)$, with known frame offset ζ.

The dual-plane ensemble correlation can be calculated using these signals, $I_\mathrm{f}(\mathbf{x}_0, t)$ and $I_\mathrm{b}(\mathbf{x}_\zeta, t)$, as

$$R_\mathrm{fb}(\zeta) = \frac{\sigma_\mathrm{fb}(\zeta)}{\sigma_\mathrm{f}(0)\,\sigma_\mathrm{b}(\zeta)}. \tag{1}$$

Here, $\sigma_\mathrm{fb}(\zeta)$ represents the covariance of the two brightness signals from the two different planes with a frame offset of ζ. It is defined as

$$\sigma_\mathrm{fb}(\zeta) = \sum_{k=0}^{N-1} \left[I_\mathrm{f}(\mathbf{x}_0, t_k) - \overline{I}_\mathrm{f} \right] \left[I_\mathrm{b}(\mathbf{x}_\zeta, t_{k+\zeta}) - \overline{I}_\mathrm{b} \right]. \tag{2}$$

In addition, $\sigma_\mathrm{f}(0)$ and $\sigma_\mathrm{b}(\zeta)$ are the standard deviations of each signal,

$$\sigma_\mathrm{f}(0) = \sqrt{\sum_{k=0}^{N-1} \left[I_\mathrm{f}(\mathbf{x}_0, t_k) - \overline{I}_\mathrm{f} \right]^2} \tag{3}$$

and

$$\sigma_\mathrm{b}(\zeta) = \sqrt{\sum_{k=0}^{N-1} \left[I_\mathrm{b}(\mathbf{x}_\zeta, t_{k+\zeta}) - \overline{I}_\mathrm{b} \right]^2}. \tag{4}$$

Here, N is the number of the frames, and $\overline{I}_\mathrm{f}$ and $\overline{I}_\mathrm{b}$ are the mean values of each signal. Using the dual-plane ensemble correlation for positive and negative frame offsets, we can determine the optimal frame offset, i.e., how many frames before or after the current frame does the particle appear in the other plane. That is, the optimal frame offset field Δf_f is determined pixelwise as $\Delta f_\mathrm{f} = \zeta_\mathrm{max}$, where ζ_max is the frame offset yielding the maximum R_fb. The same procedure can be conducted for R_bf, and thus Δf_b is obtained.

The out-of-plane velocity fields $w(\mathbf{x})$ can be determined using Δf as

$$w_\mathrm{f}(\mathbf{x}) = \frac{\Delta z}{\Delta t} \Delta f_\mathrm{f}(\mathbf{x})^{-1} \quad \text{and} \quad w_\mathrm{b}(\mathbf{x}) = -\frac{\Delta z}{\Delta t} \Delta f_\mathrm{b}(\mathbf{x})^{-1} \tag{5}$$

for the foreside and backside planes, respectively. Because the dual-plane ensemble correlation allows pixelwise frame offset fields Δf to be measured, the out-of-plane velocity fields w can be measured up to a maximum velocity of $\pm|\Delta z/\Delta t|$ with single-pixel resolution.

3 Implementation and experiment

3.1 Experiment

To examine the algorithm of dual-plane ensemble correlation, we conducted the test experiment schematically illustrated in Fig. 2. A rotating flow driven by an impeller was used as the measurement target. An acrylic cylinder with a diameter of 200 mm was used as the fluid vessel and inserted into a rectangular vessel to act as a water jacket. Water was used as the test fluid and filled the vessel up to a height of 150 mm. Particles consisting of silver-coated hollow glass spheres (mean diameter 10 μm, density 1.4 g/cm³, *Dantec Dynamics*) were seeded into the fluid as tracer particles. The impeller, comprising four wings with an attack angle of 30°, was located at the center of the cylinder, and the bottom of it was placed at half the height of the fluid ($y = 75$ mm). The impeller rotated at a constant angular velocity of 30 rpm in the clockwise direction, which was sufficiently fast to induce three-dimensional flows while keeping the fluid surface flat.

Two adjoining laser sheets, a continuous wave (CW) blue laser (wavelength 450 nm) and a CW red laser (wavelength 640 nm), illuminated two parallel planes with a depth offset of $\Delta z = 1$ mm. Each of the two lasers formed a 1-mm-thick laser sheet using a cylindrical lens, and they illuminated vertical cross-sections at $z = -40 \pm 1$ mm without overlapping. The depth offset and the thicknesses of the two laser sheets were carefully
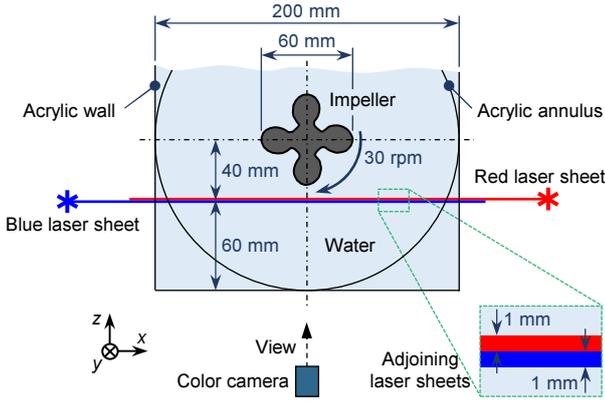
Fig. 2 Top view of the experimental setup.

Fig. 3 Pre-processing to measure the in-plane displacement vector fields at the two planes: **a** original color image; **b** foreside (left) and backside images (right) corresponding to the enclosed region of **a**; **c** overall views of displacement vector fields $d\mathbf{x}_f$ (left) and $d\mathbf{x}_b$ (right). **a** and **b** show cropped regions of 300×200 pixels and 80×60 pixels, respectively. The images in **b** are colored for better visibility. The color contours of **c** show the absolute displacements $|d\mathbf{x}|$, and every hundredth vector in the x and y directions is superposed as a black arrow.

adjusted to vary less than 10% throughout the field of view in the present study, as these mechanical settings directly affect the accuracy of the out-of-plane velocity. A CMOS color camera with a resolution of 0.1 mm/pixel was placed perpendicular to the planes. Continuous image acquisition was performed at 90 fps for 200 s, and 18,000 images were recorded as color images $\mathbf{I}_{org}$.

3.2 Pre-processing

The particles appearing in the original images $\mathbf{I}_{org}$ (Fig. 3a) first need to be separated by color into foreside $\mathbf{I}_f$ and backside images $\mathbf{I}_b$. Because of the colors of the laser sheets, blue-dominant and red-dominant pixels are regarded as indicating the particles existing in each plane, and are hence assigned to $\mathbf{I}_f$ and $\mathbf{I}_b$. This separation is formulated pixelwise as

$$I_f(x,y) = \begin{cases} I_{org}(x,y) & \text{if } I_{org}(x,y) = B_{org}(x,y) \\ 0 & \text{otherwise} \end{cases} \quad (6)$$

and

$$I_b(x,y) = \begin{cases} I_{org}(x,y) & \text{if } I_{org}(x,y) = R_{org}(x,y) \\ 0 & \text{otherwise} \end{cases}. \quad (7)$$

Here, I_{org} represents the brightness value at (x,y), defined as the maximum of the three brightness values of red (R_{org}), green (G_{org}), and blue (B_{org}). The backside image $\mathbf{I}_b$ contains defective pixels due to particles assigned to the foreside image $\mathbf{I}_b$ since the two planes were visualized by a single camera. Such defects were therefore padded by Gaussian blurring after background subtraction; the results are shown in Fig. 3b.

SP-PIV analysis (Westerweel et al. 2004) is then performed on the sets of $\mathbf{I}_f$ and $\mathbf{I}_b$ individually to obtain the in-plane displacement vector fields, $d\mathbf{x}_f$ and $d\mathbf{x}_b$, at the two planes. According to the earlier works (Westerweel et al. 2004; Ozawa et al. 2020; Nonomura et al.
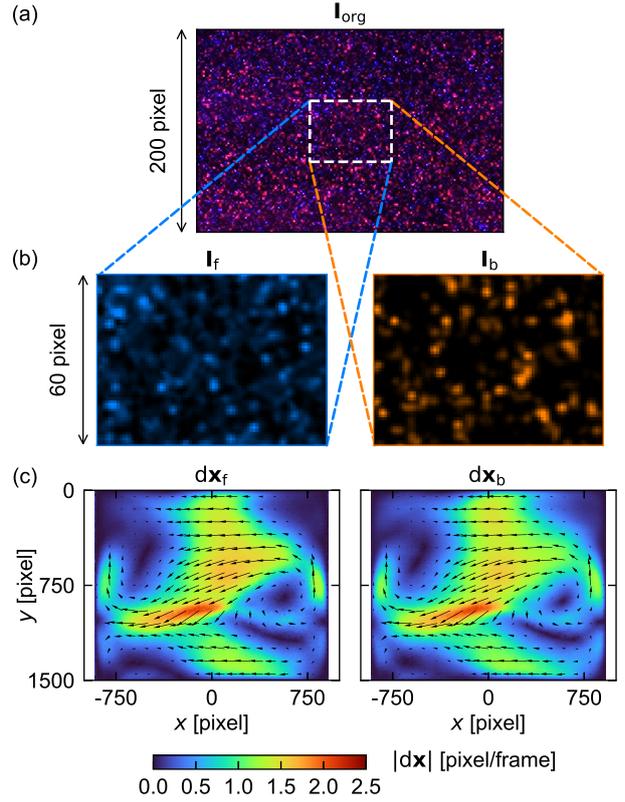
2020), SP-PIV requires a number of sequential images to achieve statistically converged velocity fields, while the number depends on the measurement conditions; it is typically, from a few thousand to ten thousand. In the present study, similar to the previous studies, at least a few thousands of sequential images were required for the convergence in the present study, and 16,000 consecutive images were used for the ensemble correlation to acquire fully converged velocity fields $d\mathbf{x}_f$ and $d\mathbf{x}_b$ with single-pixel resolution. The accuracy of the displacements was improved to sub-pixel level by fitting Gaussian-peaks to the correlation maps. The results are shown in Fig. 3c. The two flow fields show similar patterns but with considerable differences due to the small differences in positions relative to the impeller, placed at $y = 750$ pixel. Please note that the accuracy of the in-plane displacement can be improved by using several time steps for SP-PIV, however, we only adopted one frame offset at this moment to match the frame

offset used in the subsequent analysis for the sake of simplicity.

3.3 Out-of-plane velocity determination

Assuming that the in-plane velocity hardly changes between the two planes, a position $\mathbf{x}_\zeta$ on one plane is determined by tracking the particle trajectory on the other plane as

$$\mathbf{x}_\zeta = \mathbf{x}_0 + \text{sgn}(\zeta) \sum_{l=1}^{|\zeta|} d\mathbf{x}\left(\mathbf{x}_{\text{sgn}(\zeta)(l-1)}\right), \tag{8}$$

where $\text{sgn}(\cdot)$ denotes the signum function. As $\mathbf{x}_\zeta$ is determined with sub-pixel accuracy, the weighted averages of the displacement vectors $d\mathbf{x}$ and brightness values I of the four nearest pixels are used as the representative values at position $\mathbf{x}_\zeta$, as shown in Fig. 1. The dual-plane ensemble correlation is calculated only along the particle trajectory, and thus the computational time for searching ± 50 frames is almost equivalent to that required for SP-PIV searching 10×10 pixels.

Results of the most likely frame offset fields and out-of-plane velocity fields are shown in Fig. 4a and b, respectively. Here, ten thousands of sequential images were required at most for the convergence of the frame offset fields, which is a larger number than that required for the convergence of the in-plane velocity fields, typically a few thousand. The frame offset fields in Fig. 4a have an approximately inverse sign relationship. The resultant out-of-plane velocity fields in Fig. 4b are quite similar to each other, as the two planes are adjoining in the present study with a depth offset of $\Delta z = 1$ mm. For comparison, the mean out-of-plane velocity field measured by the conventional PIV employing the direct cross-correlation method is shown in Fig. 4c. This was obtained by stacking the mean velocity fields in the x-z planes at different y positions every 10 mm from $y = 5$ to 145 mm. The spatial resolutions in the x and y directions are 20 pixels ($= 2$ mm) and 100 pixels ($= 10$ mm), respectively. The velocity fields in Fig. 4b show good accordance with those in Fig. 4c in terms of the outline and magnitude, while retaining single-pixel resolution.

4 Summary and outlook

A novel method determining the out-of-plane velocity component has been developed as an extension of SP-PIV. The proposed method, called dual-plane ensemble correlation, uses the ensemble correlation of SP-PIV across two planes illuminated by two differently colored laser sheets. This enables the most likely frame offset
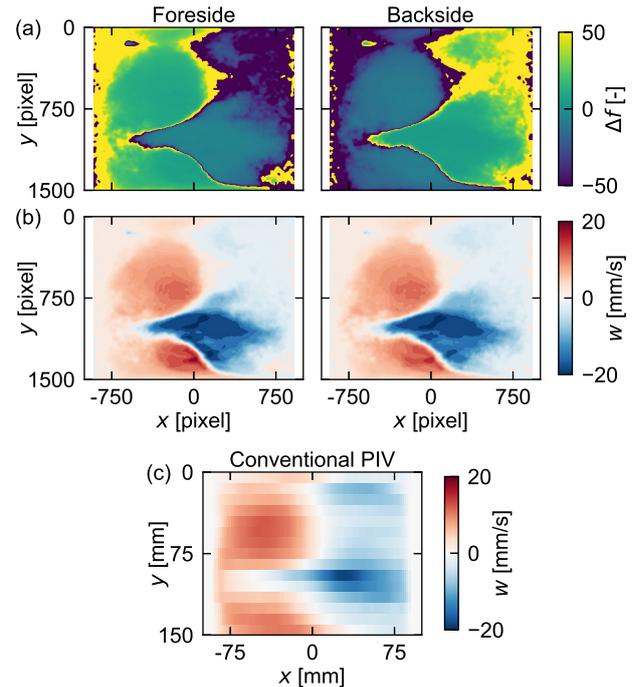

Fig. 4 a Frame offset fields of the foreside (left) and backside (right) planes, and **b** the corresponding out-of-plane velocity fields. **c** Out-of-plane velocity fields measured by conventional PIV at different horizontal planes.

and the out-of-plane velocity field to be determined. In addition to the in-plane velocity fields in the two planes acquired by the color image separation and SP-PIV, the out-of-plane velocity fields can be determined with single-pixel resolution using only a single-color camera. The method was successfully applied to a test experiment consisting of a rotating flow induced by an impeller and validated with conventional PIV.

Although the ability of the proposed method to make 3C velocity field measurements was demonstrated, some options for further refinements exist. For instance, the maximum magnitude of the out-of-plane velocity fields in Figs. 4a and b seem to be overestimated. This overestimation originates from the velocity resolution of the proposed method. Because velocity fields w are inversely proportional to frame offset Δf, the velocity resolution decreases as the out-of-plane velocity increases. In the present case, the frame offsets $\Delta f = 1, 2, 3 \dots 50$ correspond with out-of-plane velocities of $w = 90, 45, 22.5 \dots 1.8$ mm/s. The velocity resolution could tentatively be improved by adopting a larger depth offset; however, resolution in frame offset needs to be improved using methods such as Gaussian-peak fitting to determine in-plane displacements with sub-pixel accuracy in planar PIV. Iterative optimization by searching for sub-frame shifts around the optimal frame offset may solve this problem. Alternatively, an increase in

the number of visualized planes may allow accurate frame offsets to be estimated more flexibly because the combinations of planes that could be used to compute dual-plane ensemble correlation would increase. In mechanical aspects, it is necessary to determine optimal settings of laser sheets which may depend on measurement conditions in terms of beam shape, thickness, and offset.

In contrast to conventional PIV, ensemble correlation does not require spatial correlation, and thus it may be a robust approach in multiphase flows containing additional dispersed phases, e.g., gas and solid fractions. Because the 3C velocity fields at the two adjoining cross-sections can be quantified by the present method, velocity gradients in both the depth and in-plane directions can be computed. That is, all nine components of the velocity gradients can be computed, pixel by pixel.

References

Cenedese A, Paglialunga A (1989) A new technique for the determination of the third velocity component with PIV. Exp Fluids. 8(3):228–230

Gharib M, Raffel M, Ronneberger O, Kompenhans J (1995) Feasibility study of three-dimensional PIV by correlating images of particles within parallel light sheet planes. Exp Fluids. 19(2):69–77

Kähler CJ, Scholz U, Ortmanns J (2006) Wall-shear-stress and near-wall turbulence measurements up to single pixel resolution by means of long-distance micro-PIV. Exp Fluids. 41(2):327–341

Nonomura T, Ozawa Y, Ibuki T, Nankai K, Komuro A, Nishida H, Marios K, Kubo N, Kawabata H (2020) Single-pixel particle image velocimetry for characterization of dielectric barrier discharge plasma actuators. AIAA journal. 58(11):4952–4957

Ozawa Y, Ibuki T, Nonomura T, Suzuki K, Komuro A, Ando A, Asai K (2020) Single-pixel resolution velocity/convection velocity field of a supersonic jet measured by particle/schlieren image velocimetry. Exp Fluids. 61:1–18

Scharnowski S, Hain R, Kähler CJ (2012) Reynolds stress estimation up to single-pixel resolution using PIV-measurements. Exp Fluids. 52(4):985–1002

Westerweel J, Geelhoed P, Lindken R (2004) Single-pixel resolution ensemble correlation for micro-PIV applications. Exp Fluids. 37(3):375–384